Fluorescent *J*-type Aggregates and Thermotropic Columnar Mesophases of Perylene Bisimide Dyes

Frank Würthner,*[a] Christoph Thalacker,[a] Siegmar Diele,[b] and Carsten Tschierske[c]

Abstract: A series of perylene tetracarboxylic acid bisimides **3a–e** bearing 3,4,5-tridodecyloxyphenyl substituents on the imide N atoms and zero, two, or four phenoxy-type substituents in the bay positions of the perylene core were synthesized. From investigations of their spectroscopic properties and aggregation behavior in low-polarity solvents by absorption and fluorescence optical spectroscopy, not only were these compounds found to form fluorescent *J*-type aggregates, but also binding constants for aggregation could be derived which reflect the number and steric demand of the phenoxy substituents for bisimides **3a–d**. In the pristine state, **3a–d** form thermotropic hexagonal columnar mesophases which exist over a broad temperature range from below −30 °C to over 300 °C. For the tetraphenoxy-substituted compound **3e**, however, a layered crystalline structure was found. This difference in behavior can be explained by the concept of microphase segregation of the aromatic cores of the molecules and the alkyl chains at the periphery. The high stability and bright fluorescence of the mesophase of several of the compounds make them promising for applications as polarizers or components in (opto)electronic devices.

Keywords: dye aggregates · fluorescence · liquid crystals · perylene dyes · supramolecular chemistry

Introduction

The formation of structurally defined assemblies of functional building blocks with distinctive optical and electrochemical properties offers great opportunities for preparing new materials.[1] Thus, by control of the noncovalent interactions of photo- and redox-active dye molecules, extended superstructures up to mesophase materials may be derived. Recently we have investigated the hierarchical self-organization of core-substituted perylene bisimide–melamine assemblies by hydrogen bonding and π–π interactions to mesoscopic fluorescent strands.[2] With the original intention of studying the influence of the substituents on the perylene core on these π–π interactions, we synthesized a series of five perylene bisimide dyes bearing mesogenic 3,4,5-tridodecyloxyphenyl substituents[3] at the imide N atoms and different numbers (0, 2, 4) of phenoxy substituents in the bay regions of the perylene core. We discovered that four of these compounds formed hexagonal columnar mesophases over a very broad range of temperature. Until now, only a few thermotropic[4] and lyotropic[5] liquid-crystalline (LC) perylene bisimides have been described, none of which bears substituents in the bay positions. Other mesogenic perylene derivatives comprise Diels–Alder adducts of 3,5-dioxotriazoles with dialkylperylenes[6] and coronene bisimides.[7]

In this contribution we report on the spectroscopic and electrochemical properties of the new perylene bisimide dyes **3a–e** (Scheme 1), their aggregation in low-polarity solvents, and their thermotropic behavior in the pristine state as investigated by absorption and fluorescence optical spectroscopy, optical polarization microscopy (OPM), differential scanning calorimetry (DSC), and X-ray scattering. From these experiments, *J*-type fluorescent aggregates and thermotropic columnar mesophases were found to exist over a broad temperature range from below −30 °C to over 300 °C.

Results

Perylene bisimides **3a–e** were synthesized in good yields from the corresponding bisanhydrides **1a–e**[8] by condensation with 3,4,5-tridodecyloxyaniline (**2**)[9] in quinoline with zinc acetate as a Lewis acid catalyst (Scheme 1). Purification was achieved either by dissolving the crude product in

[a] Priv.-Doz. Dr. F. Würthner, C. Thalacker
Abteilung Organische Chemie II, Universität Ulm
Albert-Einstein-Allee 11, 89081 Ulm (Germany)
Fax: (+49) 731-502-2840
E-mail: frank.wuerthner@chemie.uni-ulm.de

[b] Dr. S. Diele
Institut für Physikalische Chemie
der Martin-Luther-Universität Halle-Wittenberg
Mühlpforte 1, 06108 Halle/Saale (Germany)

[c] Prof. C. Tschierske
Institut für Organische Chemie
der Martin-Luther-Universität Halle-Wittenberg
Kurt-Mothes-Strasse 2, 06120 Halle/Saale (Germany)

  0947-6539/01/0710-2245 $ 17.50+.50/0

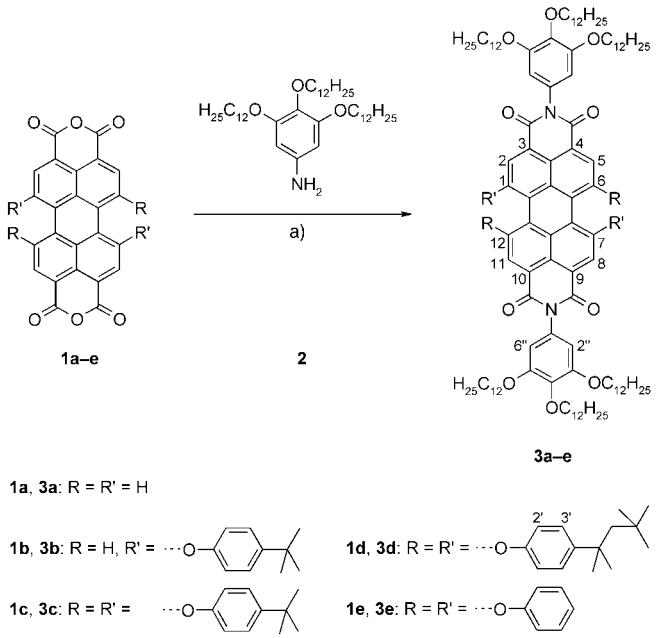

Scheme 1. Synthesis of perylene bisimides **3a–e**. a) Zinc acetate, quinoline, Ar, 180 °C, 3 h, 69–98 %.

dichloromethane and precipitating it by adding methanol, or by column chromatography.

The absorption spectra of **3a–e** are characteristic for perylene bisimides bearing zero, two, or four phenoxy substituents in the bay positions, respectively (Figure 1). For the unsubstituted perylene bisimide **3a** an absorption maximum at 527 nm with a strongly pronounced vibronic fine structure is observed which belongs to the electronic S_0-S_1 transition, with a transition dipole moment along the long molecular axis. The introduction of an increasing number of phenoxy substituents in the bay positions of the perylene core leads to a bathochromic shift of the absorption maximum to 546 nm for **3b** and 574–583 nm for **3c–e**. According to AM1 calculations and the crystal structure of a related dye,[10] these phenoxy substituents induce a twisting of the two naphthalene subunits in the perylene core by about 15° for two substituents (**3b**) and 25° for four substituents (**3c–e**). The resulting loss of planarity and rigidity of the perylene bisimide chromophore causes considerable line broadening and a less pronounced vibronic fine structure. For an increasing number of phenoxy substituents, a second absorption band evolves at lower wavelengths which is attributed to the electronic S_0-S_2 transition with a transition dipole moment perpendicular to the long molecular axis.[11] The good agreement of the peak positions and extinction coefficients for **3a–e** with those observed for perylene bisimides bearing other substituents on the imide nitrogen is explained by the presence of nodes in the HOMO and LUMO at this position.[12]

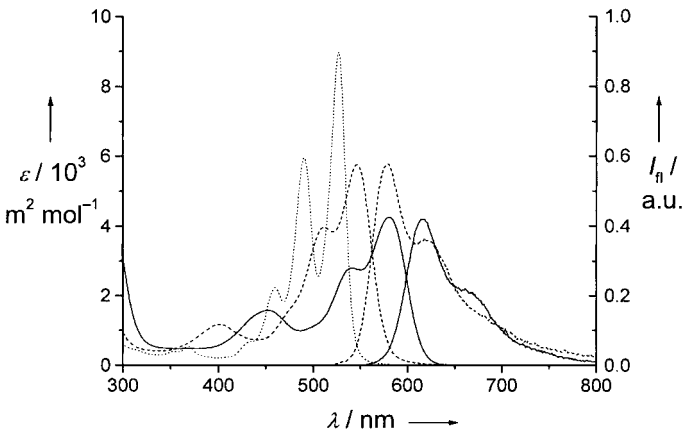

Figure 1. UV/Vis absorption and fluorescence spectra of perylene bisimides **3a** (dotted line), **3b** (broken line) and **3c** (solid line) in CH_2Cl_2. The excitation wavelength was 510 nm (**3b**) and 530 nm (**3c**).

Surprisingly, the fluorescence quantum yields for **3a–e** are not close to unity as for most perylene bisimides, but much lower (Table 1). For bisimide **3a**, no fluorescence is observed,[13] whereas for **3b–e** the fluorescence quantum yield increases with the number and electron donor quality of the phenoxy substituents. The fluorescence peaks obtained for the fluorescent perylene bisimides **3b–e** in dichloromethane are mirror images of the S_0-S_1 absorption band. Their peak positions and vibronic fine structure correspond well to those

Table 1. Peak positions of absorption (λ_a) and emission (λ_e) maxima (CH_2Cl_2), fluorescence quantum yields (Φ_f, CH_2Cl_2), binding constants K (MCH, methylcyclohexane) and Gibbs binding energies ΔG^0_{298} (MCH) for perylene bisimides **3a–e**.

compound	λ_a [nm]	λ_e [nm]	Φ_f	K [L mol^{-1}]	$-\Delta G^0_{298}$ [kJ mol^{-1}]
3a	527	–	0	1.5×10^7	40.9
3b	546	578	0.02	6.3×10^5	33.1
3c	580	616	0.21	1.2×10^5	29.0
3d	583	617	0.23	9.0×10^3	22.6
3e	574	609	0.08	1.2×10^4	23.3

Abstract in German: *Die Synthese von fünf Perylentetracarbonsäurebisimiden (**3a–e**) mit 3,4,5-Tridodecyloxyphenyl-Substituenten an den Imid-Stickstoffatomen und einer unterschiedlichen Anzahl (0, 2, 4) verschiedener Phenoxy-Substituenten in den „Bay"-Positionen des Perylengrundgerüsts wird beschrieben. Die optischen Eigenschaften und das Aggregationsverhalten dieser Farbstoffe in unpolaren Lösungsmitteln wurden durch UV/Vis-Absorptions- und Fluoreszenzspektroskopie charakterisiert, welche die Ausbildung fluoreszierender J-Aggregate belegen. Darüberhinaus konnten die Bindungskonstanten für den Aggregationsprozeß bestimmt werden, die die Anzahl und den sterischen Anspruch der Phenoxysubstituenten in Verbindung **3a–d** widerspiegeln. In Substanz bilden die Bisimide **3a–d** thermotrope hexagonale columnare Mesophasen, die über einen breiten Temperaturbereich von unter −30 °C bis über 300 °C stabil sind. Für die tetraphenoxy-substituierte Verbindung **3e** wurde hingegen eine kristalline Schichtstruktur gefunden. Dieser Unterschied kann durch das Konzept der Mikrophasen-Segregation der aromatischen Grundgerüste der Moleküle und der Alkylgruppen an der Peripherie erklärt werden. Die hohe Stabilität und die intensive Fluoreszenz einiger dieser Verbindungen, auch in der Mesophase, erscheinen vielversprechend für Anwendungen als Polarisatoren oder in (opto)elektronischen Bauelementen.*

0947-6539/01/0710-2246 $ 17.50+.50/0 *Chem. Eur. J.* **2001**, *7*, No. 10

of known perylene bisimides with a similar substitution pattern at the bay positions.[7, 8, 11, 14]

Further insight into the electronic properties of these dyes was gained by cyclic voltammetry. Two reversible reduction waves were detected at potentials of -0.98 and -1.19 V versus Fc/Fc^+ (Fc = ferrocene) for **3a** and at about -1.1 and -1.3 V for **3b**–**e** (Table 2). These values are in good agreement with literature data for perylene bisimides with zero and four phenoxy substituents in the bay positions;[15] this also reflects the greater electron density at the perylene core for **3b**–**e** than for **3a**. All the compounds investigated underwent an irreversible oxidation at potentials above $+0.9$ V (vs. Fc/Fc^+) which we attribute to oxidation of the trialkoxyphenyl substituents. For **3b**–**e**, this signal was superimposed by a reversible oxidation peak at $+1.05$ V for **3b** and about $+0.85-0.9$ V for **3c**–**e** which stems from the formation of the perylene bisimide radical cation.[15]

Table 2. Electrochemical properties of perylene bisimides **3a**–**e** in CH_2Cl_2. Scan rate $0.1\,V\,s^{-1}$, concentration $\approx 10^{-3}\,mol\,L^{-1}$, supporting electrolyte NBu_4PF_6 ($0.1\,mol\,L^{-1}$).

Compound	$E_{1/2}$ [V vs. Fc/Fc^+] X^-/X^{2-}	X/X^-	X/X^+	Irrev. ox.
3a	-1.19	-0.98	–	>0.9
3b	-1.29	-1.11	1.05	>0.9
3c	-1.25	-1.09	0.88	>0.9
3d	-1.30	-1.12	0.86	>0.9
3e	-1.30	-1.10	0.89	>0.9

The evidence of facile oxidation of the tridodecyloxyphenyl groups and the influence of the number of phenoxy substituents on the redox potentials of the perylene bisimide core could explain the observed fluorescence properties. Thus, if the HOMO is located on the trialkoxyphenyl subunit (as in **3a** and **3b**) photo-excitation of the perylene bisimide chromophore might be followed by a rapid intramolecular electron transfer leading to a nonemissive charge-separated excited state. For the more electron-rich tetraphenoxy-substituted perylene bisimides **3c**–**e** (HOMO on the perylene bisimide core), however, fluorescence from the excited singlet state of the chromophore is observed. From the rotational mobility of the trialkoxyphenyl unit we assume a broad distribution for its energy levels due to different degrees of electronic coupling to the imide N atoms for different twisting angles. Therefore the changes observed in the fluorescence quantum yields are quite smooth, rather than abrupt, for the series **3a**–**e**.

In contrast to their behavior in aromatic and chloroaliphatic solvents, strong aggregation of these perylene bisimide dyes takes place in low-polarity environments. The aggregation of **3a**–**e** was studied in detail by UV/Vis absorption and fluorescence spectroscopy of methylcyclohexane (MCH) solutions, which revealed pronounced changes of the optical properties upon changing concentration (Figure 2). For **3a** and **3b** (zero and two substituents in the bay region), strong $\pi-\pi$ interactions led to an almost complete loss of fine structure. The absorption spectra of the aggregated dyes agreed

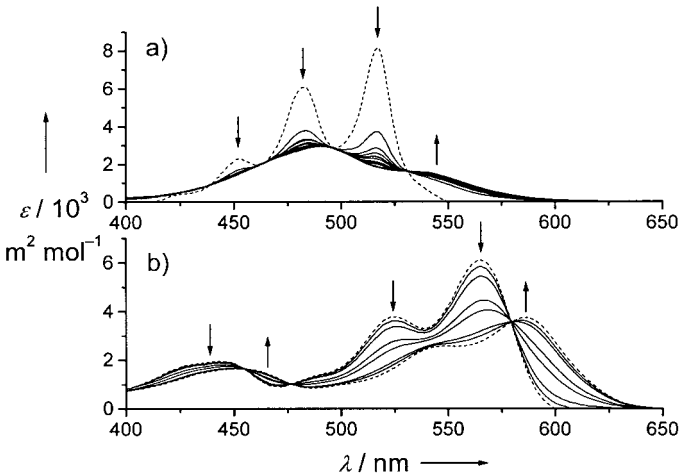

Figure 2. Concentration-dependent UV/Vis absorption spectra in MCH for a) **3a** (concentration range $10^{-7}-10^{-5}$ M) and b) **3c** (concentration range $5\times10^{-7}-10^{-4}$ M). Arrows indicate the direction of change with increasing concentration. Dotted lines represent spectra for the free and the aggregated chromophore calculated from the respective data set.

remarkably well with those reported by Graser and Hädicke for red perylene bisimide pigments in the crystalline state.[16] However, in the case of four phenoxy substituents (**3c**–**e**), the absorption spectra revealed less dramatic changes upon aggregation: The absorption maxima were red-shifted by about 20 nm, and aggregation-induced line broadening was observed, while the fine structure remained essentially the same.

For **3a**–**d**, the transition from free to $\pi-\pi$-stacked chromophores occurred at an increasing range of concentrations, which reflects the number and the steric demand of the substituents on the perylene core (Figure 3). Thus the

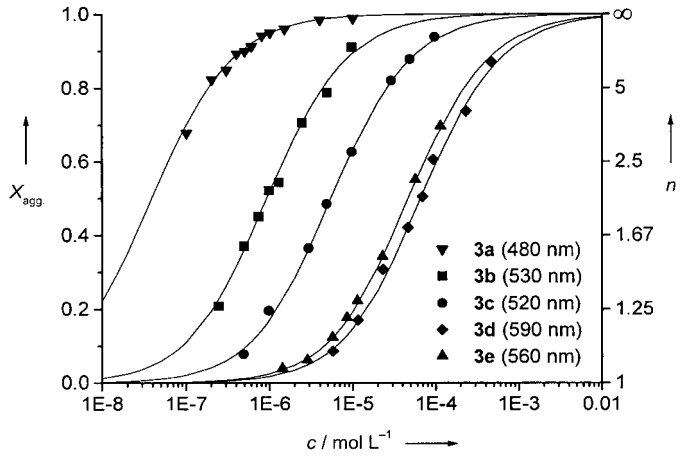

Figure 3. Fraction of aggregated molecules $X_{agg.}$ for perylene bisimides **3a**–**e** and average number of molecules per aggregate n as a function of the concentration in MCH. The curves were calculated by fitting the apparent extinction coefficients at the given wavelengths to the isodesmic or equal-K model (see Experimental Section). The aggregate size was estimated using Carothers' equation.

strongest aggregation was observed for the unsubstituted perylene bisimide **3a**, followed by **3b** bearing two *tert*-butylphenoxy substituents in the bay region. Increasing steric demand as imparted by four *tert*-butylphenoxy groups led to

even lower aggregation. Within the series **3c**–**e**, bearing four phenoxy substituents of different bulkiness, however, the results did not follow our expectations. Bisimide **3e**, which we intuitively expected to aggregate at concentrations between those for **3b** and **3c**, did not fit into the series and exhibited a much lower propensity towards π–π stacking. These observations were also matched by quantitative evaluation of the data (binding constants K and Gibbs free energies ΔG^0_{298}), achieved by fitting the data from the UV/Vis dilution studies to the isodesmic or equal-K model (Table 1) by nonlinear least-squares regression analysis (see Experimental Section).[17] The applied model assumes equal binding constants for all binding events to a one-dimensional columnar aggregate of equal components independently of the size of the aggregates, and has been applied successfully to the stacking of aromatic compounds in solution.[18] The highest binding constant is obtained for **3a** (about 10^7 L mol^{-1}); this is more than three orders of magnitude larger than that determined for **3d** and **3e** (about 10^4 L mol^{-1}). From the goodness-of-fit

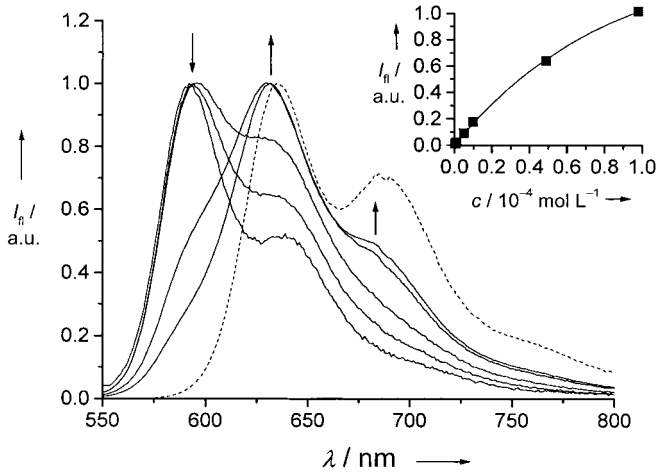

Figure 4. Normalized concentration-dependent fluorescence spectra of **3c** in MCH. Arrows indicate the direction of change with increasing concentration (concentration range 5×10^{-7}–10^{-4} M). The broken line represents the emission spectrum from a thin film of **3c** on a quartz glass slide. Inset: dependence of the fluorescence intensity I_{fl} (corrected with respect to the absorption change at the excitation wavelength) on the concentration. The data points are connected with a curve calculated by application of Beer's law to the excitation light in the sample.[20] Excitation wavelength for all spectra: 530 nm.

(Figure 3), we conclude that the behavior of **3a**–**e** is very well described by this model, and that aggregate formation occurs noncooperatively: that is, no or little change is observed in the binding constants with increasing aggregate size.[19]

Fluorescence spectroscopy of the same MCH solutions of **3b**–**e** showed a significant red shift (about 40 nm) of the emission maxima upon aggregation, with almost unaltered fine structures (Figure 4). Also, the spectra recorded from thin films on quartz glass slides closely resembled those obtained for concentrated solutions. An almost linear dependence of the fluorescence intensity on the concentration was observed after correction for the absorption change at the excitation wavelength. The deviation from linearity at higher concentrations could be described fully by the application of Beer's law to the excitation light in the sample (Figure 4, inset);[20] this indicates that the spectral changes are not merely reabsorption phenomena and that aggregation has a negligible influence on the fluorescence quantum yield Φ_f. This is a remarkable result, because aggregation often opens up new pathways for quenching of the excitation energy; this can be observed for many extended π systems, including other perylene bisimide derivatives in the solid state.[21]

The thermotropic properties of **3a**–**e** were investigated by OPM and DSC. For **3a**–**d** only one phase was found between −30 °C and the clearing point, whereas for **3e** several crystalline phases were detected. Phase transition temperatures and associated enthalpy values for **3a**–**d** are given in Table 3. When **3a** and **3c** were cooled from the isotropic liquid

Table 3. Phase transition temperatures T [°C] and transition enthalpies ΔH_t [kJ mol^{-1}] (in brackets) for perylene bisimides **3a**–**d**.

Compound	T [°C] (ΔH_t [kJ mol^{-1}])
3a	Col_{hd} 373 (8.9) I
3b	Col_{ho} 283 (6.2) I
3c	Col_{hd} 346 (15.0) I
3d	Col_{ho} 283 (23.9) I

state, a spherulitic texture which is typical for columnar mesophases was observed between crossed polarizers. Compounds **3b** and **3d** exhibited lower clearing points, and beautiful textures were obtained, reminiscent of fabrics or ferns (Figure 5). The viscosity of the LC phases increased considerably on further cooling, but no changes in the textures were observed and no glass transition could be detected by DSC. Even after six months at room temperature, no crystallization took place.

The molecular order within the LC mesophases was determined by X-ray diffraction. For **3a**–**d**, the X-ray diffraction pattern was characterized by a diffuse halo in the wide-angle region corresponding to 4–5 Å which is usually attributed to disordered alkyl chains. In the small-angle region, the unsubstituted perylene bisimide **3a** exhibited only one sharp scattering, so a particular mesophase could not be assigned to this compound (Figure 6a). However, a diffraction pattern of an oriented sample of **3a** revealed a hexagonal arrangement of the first-order reflections which confirmed a hexagonal columnar mesophase Col_h (Figure 6b). Perylene bisimides **3b** and **3c** showed two distinct scatterings in the small-angle region with a position ratio of $1:3^{0.5}$, whereas for **3d** three peaks at $1:3^{0.5}:2$ were observed. Therefore, a hexagonal columnar lattice can be assigned to these compounds also. As **3b** and **3d** exhibited an additional sharp scattering in the wide-angle region corresponding to an intracolumnar distance of 3.7 and 4.5 Å, respectively, an ordered hexagonal columnar mesophase Col_{ho} prevails in these compounds, whereas the absence of this peak implies a disordered hexagonal columnar mesophase Col_{hd} in **3a**,**c** (Figure 6). This difference is also manifest in the similarity of the clearing points and optical textures under crossed polarizers for **3a**,**c** and **3b**,**d**, respectively. The lattice parameter a_{hex}

0947-6539/01/0710-2248 $ 17.50+.50/0 *Chem. Eur. J.* **2001**, *7*, No. 10

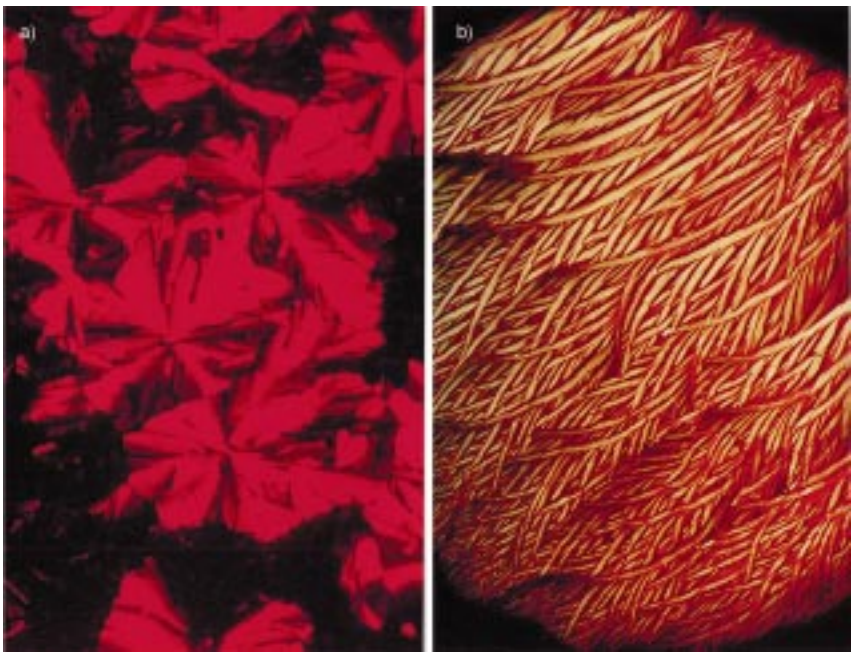

Figure 5. Optical textures of the hexagonal columnar mesophases of a) **3a** and b) **3b**, as obtained by cooling from the isotropic melt (crossed polarizers) at room temperature. Image size: a) 0.70 mm × 0.46 mm, b) 1.40 mm × 0.92 mm.

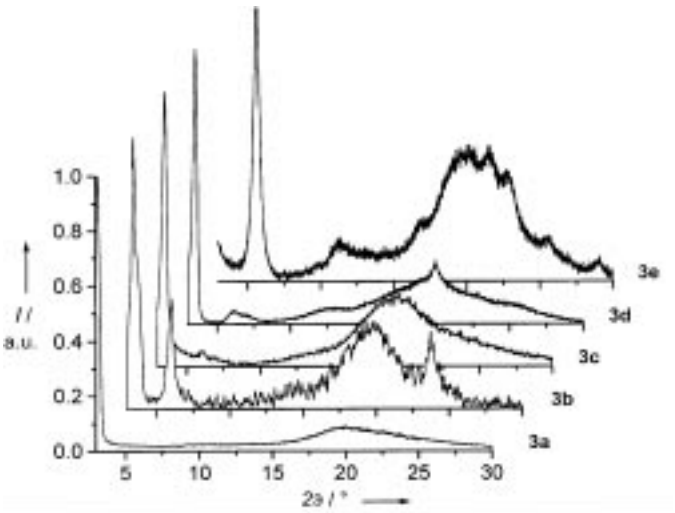

Figure 6. Top: X-ray diffraction patterns of **3a**–**e** after heating them above the clearing point and cooling to room temperature. Bottom: X-ray diffraction pattern of an oriented sample of **3a**, showing a hexagonal arrangement of the first-order diffraction peaks.

decreases progressively from **3a** to **3d**, from 32.5 to 28.7 Å (Table 4).

The X-ray diffraction pattern of **3e** at room temperature also exhibited a diffuse halo in the wide-angle region, where it was superimposed by several sharper reflections. At lower angles, three distinct scatterings were observed (position ratio 1:2:3). Hence, we conclude that a highly disordered crystalline layered structure prevails in **3e**, with a layer spacing of about 16 Å.

Discussion

Once the occurrence of columnar mesophases has been established for **3a**–**d**, the question arises of how the molecules are packed within these superstructures, especially since the hexagonal lattice constants a_{hex} are quite small (Table 4) compared with the molecular dimensions and decrease even further with increasing steric demand of the bay substituents. As estimated from molecular modeling (*CAChe3.2* MM2 force field),[22] the long molecular axis of **3a**–**e** amounts to 54 Å, with the alkyl chains in an all-*trans* conformation. The difference in behavior between **3e** and **3a**–**d** is also of interest.

To address these questions the typical procedure is to develop a packing model for the columnar mesophase and then match it with crystallographic and spectroscopic data. For the packing of flat aromatic molecules, a set of rules established by Hunter and Sanders[23] has been used successfully to describe the behavior of discotic liquid crystals.[24] As these authors pointed out, for highly polar compounds such as the given bisimides, charge–charge interactions have a dominating influence on the packing geometry. Calculation of the electrostatic surface potential for **3a**–**e** (*PC SPARTAN Pro*, AM1 force field)[25] reveals an alternating pattern of distinct areas of negative potential at the

Table 4. Hexagonal lattice parameter a_{hex} [Å] and intracolumnar repeat distance c [Å] for perylene bisimides **3a**–**d** and layer spacing d [Å] for perylene bisimide **3e** as determined from X-ray scattering at ambient temperature.

Compound	Mesophase	a_{hex} [Å][a]	c [Å]
3a	Col_{hd}	32.5	–
3b	Col_{ho}	29.3	3.7
3c	Col_{hd}	29.0	–
3d	Col_{ho}	28.7	4.5
3e	K	15.6	–

[a] **3e**: d [Å].

  0947-6539/01/0710-2249 $ 17.50+.50/0

trioxyphenyl unit and the imide oxygens and of positive potential in the perylene core. Consequently, for adjacent π–π stacked molecules, repulsion between like charges and attractive interactions between unlike charges afford rotational offsets within the column and/or offsets along the long molecular axis (Figure 7). In the case of flat perylene bisimides such as **3a**, both displacements are indeed observed in single crystals of related perylene bisimide dyes.[16] As a hexagonal columnar LC phase requires a circular column cross-section, we favor the model of rotational disorder around the column axis for **3a** in order to compensate for the very different dimensions of its short (9 Å) and long (54 Å) molecular axes.

For **3b**–**e**, the phenoxy substituents in the bay positions afford much more circular central units although, because of their bulkiness, these phenoxy substituents prevent close contacts of the π systems without longitudinal (or transverse) offsets between adjacent molecules. To estimate this steric influence, the following calculations were performed. Two geometry-optimized molecules (*CAChe 3.2*, MM2 force field;[22] the dodecyl chains were reduced to methyl groups) kept in a rigid conformation were oriented in a parallel manner. One molecule was held at a fixed position in space, while the other was moved over it in the longitudinal and transverse direction at a distance of 3.7 Å for **3b** and 4.7 Å for **3c**–**e**. For all compounds, the energy minimum was found for a longitudinal offset varying from 4.2 Å (corresponding to one benzene ring) for **3b** to 6 Å for **3d**, and a transverse slip close to zero. Different starting geometries led to the same minimum. To assign the minimum energy conformation, a geometry optimization (*CAChe 3.2*, MM2 force field) was performed again, which left the longitudinal and transverse slip essentially unchanged. The calculated distance between the perylene cores varied with the increasing steric demand of the phenoxy substituents in the bay positions from 3.7 Å (**3b**) to 4–5 Å (**3c**–**e**), with the phenoxy substituents of the upper molecule filling the space between those of the lower one. These values are in excellent agreement with those obtained from X-ray diffraction for the intracolumnar repeat distance *c* of **3b** (3.7 Å) and **3d** (4.5 Å). From the longitudinal offset, a tilted stacking of the molecules can be expected at 35–45° to the column axis (Figure 7). This tilted arrangement of the perylene bisimides within the column implies a lower aspect ratio of the column cross-section, which favors the formation of hexagonal mesophases (as observed for **3a**–**d**) rather than rectangular or oblique mesophases.

The difference in behavior of **3e** can be explained by the concept of microphase segregation.[26] For **3a**–**d**, no additional lateral π–π interactions are possible for the columnar aggregates, because the alkyl chains on the periphery of the columns and the bulky *tert*-butyl and *tert*-octyl groups on the phenoxy substituents in **3b**–**d** limit further packing of the π systems within a second dimension. For **3e**, columnar motifs are also likely, but here additional lateral π–π interactions become possible by interdigitation of the phenoxy substituents which leads to a layered crystalline structure with a layer spacing of about 16 Å; this corresponds well with the short molecular axis of **3e**. From the unexpectedly low binding constant for **3e** (Table 1), we conclude that its aggregate in solution might also exhibit some differences from those of **3a**–**d**.

The packing model of Figure 7 is also in accordance with the spectral data obtained from the aggregation studies in MCH. In their extensive phenomenological study, Graser and Hädicke tried to correlate the solid-state absorption spectra of perylene bisimide crystals with the crystal structure.[16] On the basis of absorption properties, they distinguished three classes of pigments. "Red pigments" have a rather small overlap of the π systems in the crystal, that is a comparatively large shift of the chromophores with respect to each other, and "black pigments" exhibit a large overlap. Within the crystals of these two pigment classes, the molecules are typically arranged in tilted stacks with a distance of 3.4–3.7 Å between the perylene planes. The third class also affords "red pigments", but the π systems are further apart because of bulkier substituents, and the absorption characteristics of the crystal are mainly those of the chromophores in solution, accompanied by line broadening and a small red shift of the absorption maxima. For the first two perylene pigment classes, Kazmaier and Hoffmann analyzed the crystallochromic properties on the basis of extended Hückel calculations.[27] From the nodal character of the HOMO and the

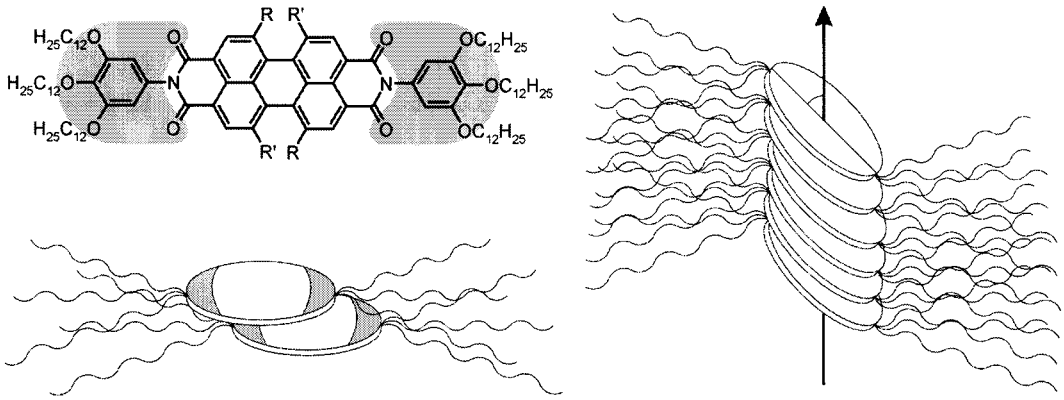

Figure 7. Model of the arrangement of **3b**–**d** in the columnar mesophase, based on electrostatic interactions between the perylene bisimide chromophores and steric demand of the substituents in the bay positions which lead to a longitudinal offset. For **3a**, a rotational offset around the column axis is more likely. Areas with a negative electrostatic surface potential are shaded gray.

  0947-6539/01/0710-2250 $ 17.50+.50/0 *Chem. Eur. J.* **2001**, *7*, No. 10

LUMO wavefunctions, they concluded that these pigments should be assigned to either the "red" or the "black" class not simply from the overlap of the perylene chromophores, but also according to their longitudinal and transverse offset within the stack. As presented above, our model predicts for compound **3b** a longitudinal slip of one benzene ring (about 4.2 Å) and almost no transverse shift. According to Kazmaier and Hoffmann, perylene bisimides with this offset within the stack belong to the "red" class, which is consistent with our spectral data (Figure 2a). The intracolumnar distance (3.7 Å) obtained for **3b** from X-ray scattering is also in accordance with the spectral properties and data from single-crystal structure analyses reported by Graser and Hädicke.[16] However, **3c–e**, with four bulky substituents, show the characteristics of the third class of perylene bisimide pigments distinguished by Graser and Hädicke (Figure 2b). Notably, for **3d** the intracolumnar distance between adjacent molecules, determined by X-ray diffraction, is 4.5 Å.

Beyond this simple classification scheme, the changes in the optical properties upon aggregation within the given series of perylene bisimides might be analyzed by exciton coupling theory.[28] Clearly the close intracolumnar spacing of **3a** and **3b** allows strong excitonic coupling of the chromophores, giving rise to the completely altered spectral fine structure, whereas this is not the case for **3c–e**.[29] Indeed, exciton coupling theory predicts a third-power relationship between the sum of the coupling energies of the transition dipoles and the distance between the dipole centers. Therefore less pronounced spectral changes for the aggregates of **3c–e** with more distant chromophores are in good agreement with this model.

The evidence of strong excitonic coupling leads to another aspect. On the basis of their different optical properties which result from different coupling modes between the chromophores, two main species of dye aggregates are distinguished in the literature: *H*-aggregates where the absorption maximum of the aggregate is blue-shifted with respect to the isolated chromophore and where fluorescence of the isolated chromophore is lost in the aggregate, and *J*-aggregates where absorption and emission maxima are red-shifted and no quenching occurs in the aggregate.[30] The common structural model for such aggregates is based on the longitudinal offset of the dye molecules and is sometimes described as the "deck-of-cards" model, where the cards represent the molecules stacked on top of each other. The angle between the molecular plane and the aggregation direction decides between the presence of an *H*- or a *J*-aggregate: above a theoretical value of 54.7° an *H*-aggregate is usually found, whereas in *J*-aggregates the molecules have slipped more with respect to each other, leading to a smaller angle.[31] The angles obtained by molecular modeling for **3b–e** (35–45°), and also supported by X-ray data, are well below this theoretical value, indicating the formation of *J*-type aggregates. This is again supported by the spectral data, as a bathochromic shift is observed in the absorption spectra of all aggregates of **3a–e**, and for **3b–e** fluorescent aggregates with a red-shifted emission maximum are found. It is noteworthy that a similar bathochromic shift of the emission detected for a perylene bisimide cyclophane was also attributed to excitonic coupling in a *J*-type aggregate.[32]

Conclusion

We have found *J*-type aggregates and columnar mesophases of perylene bisimide dyes by simple derivatization of the imide groups with mesogenic trialkoxyphenyl substituents. The most probable packing model for the hexagonal columnar mesophases of **3b–d** consists of molecules tilted at about 35–45° with respect to the column axis, whereas for **3a** a more disordered arrangement of the molecules within the column is likely. With increasing steric demand of the phenoxy substituents an increase in the longitudinal slip of the molecules and larger π–π distances between the perylene bisimide cores are observed. This permits folding and interpenetration of the disordered alkyl chains at the periphery and thus explains the decreasing hexagonal lattice parameter a_{hex} within the series **3a–d**.

For the derivatives with four phenoxy substituents in the bay region of the perylene core, the strong fluorescence observed even in the aggregated state makes these LC phases interesting for applications as polarizers or components in electroluminescent devices. Another major interest in discotic LC phases of extended π systems stems from their charge transport properties, which are desirable for photoconductors and organic semiconductors.[33] However, until now all known discotic LC systems have been p-type conducting species. As crystalline perylene bisimides exhibit n-type semiconducting properties,[34] we expect n-type charge transport within the given mesophases.

Experimental Section

Materials and methods: Solvents and reagents were purchased from Merck (Darmstadt, Germany) unless otherwise stated, and purified and dried according to standard procedures.[35] Perylene-3,4:9,10-tetracarboxylic acid bisanhydride (**1a**, Aldrich) was used as a starting material for the synthesis of 1,7-di(4-*tert*-butylphenoxy)perylene-3,4:9,10-tetracarboxylic acid bisanhydride (**1b**),[8a] 1,6,7,12-tetra(4-*tert*-butylphenoxy)perylene-3,4:9,10-tetracarboxylic acid bisanhydride (**1c**),[8b] 1,6,7,12-tetra[4-(1,1,3,3-tetramethylbutyl)phenoxy]perylene-3,4:9,10-tetracarboxylic acid bisanhydride (**1d**),[8c] and 1,6,7,12-tetraphenoxyperylene-3,4:9,10-tetracarboxylic acid bisanhydride (**1e**)[8b] according to the literature. 3,4,5-Tridodecyloxyaniline (**2**) was obtained according to ref. [9]. Column chromatography was performed on silica gel (Merck silica gel 60, 0.2–0.5 mm, 50–130 mesh). The solvents for spectroscopic studies were of spectroscopic grade and used as received (MCH was purchased from Aldrich). UV/Vis spectra were taken on a Perkin–Elmer Lambda 40P spectrometer and fluorescence spectra were measured on a SPEX Fluorolog 2 spectrofluorimeter. NMR spectra were recorded on a Bruker DRX 400 spectrometer using the proton signal of TMS or the carbon signal of the deuterated solvent as internal standard. Optical textures at crossed polarizers were obtained with a Zeiss Axiophot Pol polarization microscope equipped with a Linkam THMSG 600 hot stage and a Linkam TP 92 controller unit. DSC measurements were performed using a Perkin–Elmer DSC-7 calorimeter. Wide-angle X-ray diffractograms were obtained at room temperature on a Siemens D 500 powder diffractometer (Ni-filtered $Cu_{K\alpha}$ radiation). Samples for X-ray diffraction were prepared by heating above the clearing point and cooling to room temperature. To prepare an oriented sample, a small amount of **3a** was heated above the clearing point between two thin beryllium foils, and cooled slowly to room temperature.

General procedure for preparation of 3a–e: Each of the perylene tetracarboxylic acid bisanhydrides (**1a–e**, 1 equiv) was stirred under argon with 3,4,5-tridodecyloxyaniline **2** (2.4–3 equiv) and zinc acetate (1 equiv, Fluka) in quinoline (30 mL per mmol bisanhydride) at 180 °C for 3 h. The

reaction mixture was cooled to room temperature and poured into HCl (1M, 100 mL). The resulting violet precipitate was collected on a glass filter funnel, washed with water (50 mL) and methanol (50 mL), then purified either by dissolving the crude product in CH_2Cl_2 and precipitating it by addition of methanol or by column chromatography (silica gel, CH_2Cl_2).

***N,N′*-Di(3,4,5-tridodecyloxyphenyl)perylene-3,4:9,10-tetracarboxylic acid bisimide (3a)**: Prepared from **1a** (0.12 g, 0.3 mmol) and **2** (0.58 g, 0.9 mmol). Purified by precipitation from CH_2Cl_2. Yield: 0.44 g (89%); Col_{hd} 373 °C I; ^{1}H NMR (400 MHz, $CDCl_3$, 25 °C, TMS): $\delta = 8.42$ (d, $^3J(H,H) = 7.5$ Hz, 4H; H2,5,8,11), 7.93 (d, $^3J(H,H) = 7.4$ Hz, 4H; H1,6,7,12), 6.69 (s, 4H; H2″,6″), 4.03 (t, 4H; OCH_2), 3.81 (t, 8H; OCH_2), 1.82 (m, 4H), 1.72 (m, 8H), 1.6–1.2 (m, 108H), 0.85 (m, 18H); ^{13}C NMR (100 MHz, $CDCl_3$, 25 °C): $\delta = 162.82$, 153.68, 138.19, 133.45, 130.76, 129.72, 128.25, 125.19, 123.13, 122.72, 106.99, 73.45, 69.18, 31.98, 31.93, 30.57, 29.90, 29.86, 29.78, 29.77, 29.74, 29.72, 29.59, 29.49, 29.45, 29.40, 26.28, 26.12, 22.71, 22.67, 14.10, 14.06; UV/Vis (CH_2Cl_2): λ_{max} (ε) = 527 (89600), 490 (59500), 459 nm (22300 $mol^{-1}Lcm^{-1}$); elemental analysis (%) calcd for $C_{108}H_{162}N_2O_{10}$ (1648.5): C 78.69, H 9.91, N 1.70; found: C 78.50, H 9.81, N 1.62.

***N,N′*-Di(3,4,5-tridodecyloxyphenyl)-1,7-di(4-*tert*-butylphenoxy)perylene-3,4:9,10-tetracarboxylic acid bisimide (3b)**: Prepared from **1b** (0.34 g, 0.5 mmol) and **2** (0.97 g, 1.5 mmol). Purified by column chromatography. Yield: 0.58 g (60%); Col_{ho} 283 °C I; ^{1}H NMR (400 MHz, $CDCl_3$, 25 °C, TMS): $\delta = 9.49$ (d, $^3J(H,H) = 8.3$ Hz, 2H; H6,12), 8.51 (d, $^3J(H,H) = 8.3$ Hz, 2H; H5,11), 8.25 (s, 2H; H2,8), 7.46 (d, $^3J(H,H) = 8.8$ Hz, 4H; H3′,5′), 7.10 (d, $^3J(H,H) = 8.7$ Hz, 4H; H2′,6′), 6.53 (s, 4H; H2″,6″), 4.00 (t, 4H; OCH_2), 3.82 (t, 8H; OCH_2), 1.74 (m, 12H), 1.6–1.2 (m, 108H), 1.36 (s, 18H; *t*Bu), 0.87 (m, 18H); ^{13}C NMR (100 MHz, $CDCl_3$, 25 °C): $\delta = 163.24$, 162.92, 155.60, 153.63, 152.21, 148.51, 138.21, 133.38, 130.09, 129.74, 128.90, 128.75, 127.53, 124.74, 123.68, 123.63, 123.43, 122.08, 119.32, 106.81, 73.42, 69.02, 34.54, 31.96, 31.92, 31.42, 30.47, 29.82, 29.80, 29.72, 29.67, 29.47, 29.41, 29.36, 26.19, 26.09, 22.70, 22.67, 14.10, 14.08; UV/Vis (CH_2Cl_2): λ_{max} (ε) = 546 (57500), 511 (39600), 402 nm (11600 $mol^{-1}Lcm^{-1}$); fluorescence (CH_2Cl_2): $\lambda_{max} = 578$ nm; elemental analysis (%) calcd for $C_{128}H_{186}N_2O_{12}$ (1944.9): C 79.05, H 9.64, N 1.44; found: C 79.00, H 9.77, N 1.49.

***N,N′*-Di(3,4,5-tridodecyloxyphenyl)-1,6,7,12-tetra(4-*tert*-butylphenoxy)perylene-3,4:9,10-tetracarboxylic acid bisimide (3c)**: Prepared from **1c** (0.25 g, 0.25 mmol) and **2** (0.48 g, 0.75 mmol). Purified by precipitation from CH_2Cl_2. Yield: 0.52 g (92%); Col_{hd} 346 °C I; ^{1}H NMR (400 MHz, $CDCl_3$, 25 °C, TMS): $\delta = 8.23$ (s, 4H; H2,5,8,11), 7.24 (d, $^3J(H,H) = 8.8$ Hz, 8H; H3′,5′), 6.84 (d, $^3J(H,H) = 8.8$ Hz, 8H; H2′,6′), 6.41 (s, 4H; H2″,6″), 3.98 (t, 4H; OCH_2), 3.89 (t, 8H; OCH_2), 1.75 (m, 12H), 1.6–1.2 (m, 108H), 1.29 (s, 36H; *t*Bu), 0.87 (m, 18H); ^{13}C NMR (100 MHz, $CDCl_3$, 25 °C): $\delta = 163.61$, 156.17, 153.62, 152.75, 147.50, 138.22, 132.09, 130.12, 126.67, 122.58, 120.64, 120.06, 119.68, 119.43, 106.80, 73.44, 69.05, 34.34, 31.93, 31.90, 31.39, 30.34, 29.74, 29.67, 29.63, 29.61, 29.37, 29.36, 29.33, 29.31, 26.12, 26.07, 22.68, 22.66, 14.08; UV/Vis (CH_2Cl_2): λ_{max} (ε) = 580 (42 500), 542 (28 000), 452 nm (15 800 $mol^{-1}Lcm^{-1}$); fluorescence (CH_2Cl_2): $\lambda_{max} = 616$ nm; elemental analysis (%) calcd for $C_{148}H_{210}N_2O_{14}$ (2241.3): C 79.31, H 9.44, N 1.25; found C 78.91, H 9.27, N 1.27.

***N,N′*-Di(3,4,5-tridodecyloxyphenyl)-1,6,7,12-tetra[4-(1,1,3,3-tetramethylbutyl)phenoxy]perylene-3,4:9,10-tetracarboxylic acid bisimide (3d)**: Prepared from **1d** (0.30 g, 0.25 mmol) and **2** (0.39 g, 0.6 mmol). Purified by column chromatography. Yield: 0.55 g (89%); Col_{ho} 285 °C I; ^{1}H NMR (400 MHz, $CDCl_3$, 25 °C, TMS): $\delta = 8.18$ (s, 4H; H2,5,8,11), 7.24 (d, $^3J(H,H) = 8.7$ Hz, 8H; H3′,5′), 6.87 (d, $^3J(H,H) = 8.8$ Hz, 8H; H2′,6′), 6.40 (s, 4H; H2″,6″), 3.98 (t, 4H; OCH_2), 3.89 (t, 8H; OCH_2), 1.75 (m, 12H), 1.70 (s, 8H; *t*-oct), 1.5–1.2 (m, 108H), 1.33 (s, 24H; *t*-oct), 0.87 (m, 18H), 0.75 (s, 36H; *t*-oct); ^{13}C NMR (100 MHz, $CDCl_3$, 25 °C): $\delta = 163.57$, 156.29, 153.62, 152.45, 146.88, 138.23, 132.94, 130.16, 127.63, 122.59, 120.32, 119.56, 119.20, 106.80, 73.44, 69.21, 56.92, 38.25, 37.64, 32.25, 31.93, 31.68, 31.25, 29.73, 29.65, 29.61, 29.33, 29.28, 26.31, 25.99, 22.38, 14.21; UV/Vis (CH_2Cl_2): λ_{max} (ε) = 583 (51600), 544 (31600), 451 nm (17700 $mol^{-1}Lcm^{-1}$); fluorescence (CH_2Cl_2): $\lambda_{max} = 617$ nm; elemental analysis (%) calcd for $C_{164}H_{242}N_2O_{14}$ (2465.8): C 79.89, H 9.89, N 1.14; found: C 79.86, H 9.72, N 1.20.

***N,N′*-Di(3,4,5-tridodecyloxyphenyl)-1,6,7,12-tetraphenoxyperylene-3,4:9,10-tetracarboxylic acid bisimide (3e)**: Prepared from **1e** (0.19 g, 0.25 mmol) and **2** (0.48 g, 0.75 mmol). Purified by column chromatography. Yield: 0.35 g (69%); m.p. 243 °C; ^{1}H NMR (400 MHz, $CDCl_3$, 25 °C, TMS): $\delta = 8.22$ (s, 4H; H2,5,8,11), 7.25 (t, $^3J(H,H) = 8.0$ Hz, 8H; H3′,5′), 7.10 (t, $^3J(H,H) = 7.4$ Hz, 4H; H4′), 6.95 (d, $^3J(H,H) = 8.1$ Hz, 8H; H2′,6′), 6.41 (s, 4H; H2″,6″), 3.99 (t, 4H; OCH_2), 3.89 (t, 8H; OCH_2), 1.76 (m, 12H), 1.5–1.2 (m, 108H), 0.87 (m, 18H); ^{13}C NMR (100 MHz, $CDCl_3$, 25 °C): $\delta = 163.40$, 155.98, 155.19, 153.57, 138.20, 132.80, 130.11, 129.97, 129.51, 124.67, 122.80, 120.67, 120.21, 119.96, 106.85, 73.44, 69.06, 37.60, 31.92, 31.89, 30.34, 29.73, 29.66, 29.62, 29.60, 29.36, 29.32, 26.11, 26.06, 22.65, 14.07; UV/Vis (CH_2Cl_2): λ_{max} (ε) = 574 (51500), 535 (32500), 445 nm (16400 $mol^{-1}Lcm^{-1}$); fluorescence (CH_2Cl_2): $\lambda_{max} = 609$ nm; elemental analysis (%) calcd for $C_{132}H_{178}N_2O_{14}$ (2016.9): C 78.61, H 8.90, N 1.39; found C 78.40, H 9.02, N 1.40.

Fluorescence measurements: Fluorescence was measured with a calibrated SPEX Fluorolog 2 spectrofluorimeter, and all spectra were corrected. The fluorescence quantum yields in CH_2Cl_2 were determined for optically dilute solutions (O.D. < 0.04)[36] using *N,N′*-di(2,6-diisopropylphenyl)-1,6,7,12-tetraphenoxyperylene-3,4:9,10-tetracarboxylic acid bisimide as reference ($\Phi_{f,CHCl_3} = 0.96$)[11, 14b] and published refractive indices of the solvents.[37] The given quantum yields were averaged from values at three excitation wavelengths ($\sigma < 3\%$). All solutions were prepared from air-saturated solvents. A study of the reference perylene dye after degassing (six freeze–drying cycles at ultrahigh vacuum) showed that the influence of oxygen was negligible for the given chromophoric system. Owing to the high optical densities of the solutions required for aggregation studies in MCH, these samples were investigated using the front-face illumination technique on a 1 mm cell in order to minimize reabsorption, rather than the conventional right-angle setup.[38]

UV/Vis aggregation studies in MCH: A set of spectra of **3a–e** at different concentrations in MCH was recorded. The apparent extinction coefficients at several wavelengths were fitted by nonlinear regression analysis[17] to the isodesmic or equal-*K* model according to Equation (1), derived from ref. [18a]:

$$\varepsilon(c) = \frac{2Kc + 1 - \sqrt{4Kc + 1}}{2K^2c^2}(\varepsilon_f - \varepsilon_a) + \varepsilon_a \quad (1)$$

ε denotes the apparent extinction coefficient obtained from the spectra; ε_f and ε_a are the extinction coefficients for the free and the aggregated species, respectively; *K* is the binding constant; and *c* is the total dye concentration in the sample. The binding constants in Table 1 were averaged from values obtained for four different wavelengths ($\sigma < 15\%$).

Electrochemistry: Cyclic voltammetry was performed with a Jaissle BI POT PG 10 potentiostat in a three-electrode single-compartment cell with CH_2Cl_2 (5 mL) as solvent. Working electrode: platinum disk; counter electrode: platinum wire; reference electrode: Ag/AgCl. All potentials were internally referenced to the Fc/Fc^+ couple. The solutions were purged with argon before use. The supporting electrolyte was tetrabutylammonium hexafluorophosphate (0.1M) (Fluka), which was recrystallized twice from ethanol/water and dried in a high vacuum.

Acknowledgements

This work was supported by the Deutsche Forschungsgemeinschaft (a scholarship for C.T. within Graduiertenkolleg 328, "Molecular Organization and Dynamics at Interfaces and Surfaces"), the Ulmer Universitätsgesellschaft, the Fonds der Chemischen Industrie and the BMBF (Liebig grant to F.W.). We are indebted to Prof. Ulf Thewalt and Dipl.-Ing. Gerda Dörfner (Sektion Röntgen- und Elektronenbeugung, Universität Ulm) for carrying out WAXS experiments, to Prof. G. Ulrich Nienhaus (Abt. Biophysik, Universität Ulm) for the opportunity to use his fluorescence spectrometer and to Prof. Peter Bäuerle (Abt. Organische Chemie II, Universität Ulm) for his support.

[1] a) V. Balzani, F. Scandola, *Supramolecular Photochemistry*, Ellis Horwood, Chichester, **1991**; b) *Supramolecular Technology*, *Vol. 10* (Ed.: D. N. Reinhoudt) of *Comprehensive Supramolecular Chemistry* (Series Eds.: J. L. Atwood, J. E. D. Davies, D. D. MacNicol, F. Vögtle), Pergamon Press, Oxford, **1996**; c) S. R. Forrest, *Chem. Rev.* **1997**, *97*, 1793–1896.

[2] a) F. Würthner, C. Thalacker, A. Sautter, *Adv. Mater.* **1999**, *11*, 754–758; b) F. Würthner, C. Thalacker, A. Sautter, W. Schärtl, W. Ibach, O. Hollricher, *Chem. Eur. J.* **2000**, *6*, 3871–3886.

  0947-6539/01/0710-2252 $ 17.50+.50/0 *Chem. Eur. J.* **2001**, *7*, No. 10

[3] For a review on polycatenary or phasmidic mesogens see: H.-T. Nguyen, C. Destrade, J. Malthête, in *Handbook of Liquid Crystals*, *Vol. 2B*: *Low Molecular Weight Liquid Crystals II* (Eds.: D. Demus, J. Goodby, G. W. Gray, H.-W. Spiess, V. Vill), Wiley-VCH, Weinheim, **1998**, pp.865–885.

[4] a) R. A. Cormier, B. A. Gregg, *J. Phys. Chem. B* **1997**, *101*, 11004–11006; b) B. A. Gregg, R. A. Cormier, *J. Phys. Chem. B* **1998**, *102*, 9952–9957; c) R. A. Cormier, B. A. Gregg, *Chem. Mater.* **1998**, *10*, 1309–1319.

[5] I. K. Iverson, S.-W. Tam-Chang, *J. Am. Chem. Soc.* **1999**, *121*, 5801–5802.

[6] C. Göltner, D. Pressner, K. Müllen, H.-W. Spiess, *Angew. Chem.* **1993**, *105*, 1722–1724; *Angew. Chem. Int. Ed. Engl.* **1993**, *32*, 1660–1662.

[7] U. Rohr, P. Schlichting, A. Böhm, M. Groß, K. Meerholz, C. Bräuchle, K. Müllen, *Angew. Chem.* **1998**, *110*, 1463–1467; *Angew. Chem. Int. Ed.* **1998**, *37*, 1434–1437.

[8] a) A. Böhm, H. Arms, G. Henning, P. Blaschka (BASF AG), *DE 19547209 A1*, **1997** [*Chem. Abstr.* **1997**, *127*, 96569]; b) D. Dotcheva, M. Klapper, K. Müllen, *Macromol. Chem. Phys.* **1994**, *195*, 1905–1911; c) M. Schneider, K. Müllen, *Chem. Mater.* **2000**, *12*, 352–362.

[9] a) A. Zinsou, M. Veber, H. Strzelecka, C. Jallabert, P. Fourré, *New J. Chem.* **1993**, *17*, 309–313; b) V. Percec, C.-H. Ahn, T. K. Bera, G. Ungar, D. J. P. Yeardley, *Chem. Eur. J.* **1999**, *5*, 1070–1083.

[10] F. Würthner, A. Sautter, C. Thalacker, *Angew. Chem.* **2000**, *112*, 1298–1301; *Angew. Chem. Int. Ed.* **2000**, *39*, 1243–1245.

[11] R. Gvishi, R. Reisfeld, Z. Burshtein, *Chem. Phys. Lett.* **1993**, *213*, 338–344.

[12] a) H. Langhals, S. Demmig, H. Huber, *Spectrochim. Acta* **1988**, *44A*, 1189–1193; b) S. K. Lee, Y. Zu, A. Herrmann, Y. Geerts, K. Müllen, A. J. Bard, *J. Am. Chem. Soc.* **1999**, *121*, 3513–3520.

[13] Perylene bisimides bearing benzo crown ether substituents on the imide N atoms and no substituents in the bay positions also showed no fluorescence: H. Langhals, W. Jona, *DE 19709008 A1*, **1998** [*Chem. Abstr.* **1998**, *129*, 246520].

[14] a) H. Langhals, *Heterocycles* **1995**, *40*, 477–500, and references therein; b) G. Seybold, G. Wagenblast, *Dyes Pigm.* **1989**, *11*, 303–317; c) H. Quante, P. Schlichting, U. Rohr, Y. Geerts, K. Müllen, *Macromol. Chem. Phys.* **1996**, *197*, 4029–4044.

[15] a) J. Salbeck, H. Kunkely, H. Langhals, R. W. Saalfrank, J. Daub, *Chimia* **1989**, *43*, 6–9; b) W. E. Ford, H. Hiratsuka, P. V. Kamat, *J. Phys. Chem.* **1989**, *93*, 6692–6696; c) F. Würthner, A. Sautter, *Chem. Commun.* **2000**, 445–446.

[16] a) F. Graser, E. Hädicke, *Liebigs Ann. Chem.* **1980**, 1994–2011; b) F. Graser, E. Hädicke, *Liebigs Ann. Chem.* **1984**, 483–494; c) E. Hädicke, F. Graser, *Acta Crystallogr. Sect. C* **1986**, *42*, 189–195; d) G. Klebe, F. Graser, E. Hädicke, J. Berndt, *Acta Crystallogr. Sect. B* **1989**, *45*, 69–77.

[17] *Origin 5.0*, Microcal Software Inc., Northampton, MA, USA, **1997**.

[18] a) R. B. Martin, *Chem. Rev.* **1996**, *96*, 3043–3064; b) N. J. Baxter, M. P. Williamson, T. H. Lilley, E. Haslan, *J. Chem. Soc. Faraday Trans. 2* **1996**, *92*, 231–234.

[19] This is a typical feature of chromonic liquid crystals: J. Lydon, in *Handbook of Liquid Crystals*, *Vol. 2B*: *Low Molecular Weight Liquid Crystals II* (Eds.: D. Demus, J. Goodby, G. W. Gray, H.-W. Spiess, V. Vill), Wiley-VCH, Weinheim, **1998**, pp. 981–1007. Chromonic LCs are typically disk-shaped ionic compounds which form stacked, not micellar, aggregates in water.

[20] W. Schmidt, *Optische Spektroskopie*, VCH, Weinheim, **1994**, pp. 205–207.

[21] a) H. Langhals, S. Demmig, T. Potrawa, *J. Prakt. Chem.* **1991**, *333*, 733–748; b) C. Burgdorff, H.-G. Löhmannsröben, R. Reisfeld, *Chem. Phys. Lett.* **1992**, *197*, 358–363.

[22] *CAChe 3.2*, Oxford Molecular Ltd., Oxford, UK, **1999**.

[23] a) C. A. Hunter, J. K. M. Sanders, *J. Am. Chem. Soc.* **1990**, *112*, 5525–5534; b) C. A. Hunter, *Angew. Chem.* **1993**, *105*, 1653–1655; *Angew. Chem. Int. Ed. Engl.* **1993**, *32*, 1584–1586.

[24] E. O. Arikainen, N. Boden, R. J. Bushby, D. R. Lozman, J. G. Vinter, A. Wood, *Angew. Chem.* **2000**, *112*, 2423–2426; *Angew. Chem. Int. Ed.* **2000**, *39*, 2333–2336.

[25] *PC SPARTAN Pro*, Version 1.0.1, Wavefunction Inc., Irvine, CA, **1999**.

[26] a) A. Pegenau, P. Göring, C. Tschierske, *Chem. Commun.* **1996**, 2563–2564; b) A. Pegenau, T. Hegmann, C. Tschierske, S. Diele, *Chem. Eur. J.* **1999**, *5*, 1643–1660.

[27] P. M. Kazmaier, R. Hoffmann, *J. Am. Chem. Soc.* **1994**, *116*, 9684–9691.

[28] M. Kasha, H. R. Rawls, M. Ashraf El-Bayoumi, *Pure Appl. Chem.* **1965**, *11*, 371–392.

[29] Excitonic coupling of perylene derivatives has been investigated in several cases: a) W. E. Ford, P. V. Kamat, *J. Phys. Chem.* **1987**, *91*, 6373–6380; b) V. Bulovic, P. E. Burrows, J. A. Cronin, M. E. Thompson, *Chem. Phys.* **1996**, *210*, 1–12; c) M. A. Biasutti, S. De Feyter, S. De Backer, G. B. Dutt, F. C. De Schryver, M. Ameloot, P. Schlichting, K. Müllen, *Chem. Phys. Lett.* **1996**, *248*, 13–19; d) D. Schlettwein, H. Graaf, J.-P. Meyer, T. Oekermann, N. I. Jaeger, *J. Phys. Chem. B* **1999**, *103*, 3078–3086; e) H. Graaf, D. Schlettwein, N. I. Jaeger, *Synth. Met.* **2000**, *109*, 151–155.

[30] There is extensive literature on *H*- and *J*-aggregates since their discovery: G. Scheibe, L. Kandler, H. Ecker, *Naturwissenschaften* **1937**, *25*, 75; E. Jelly, *Nature* **1936**, *138*, 1009–1010. Two more recent reviews on these topics are: a) P. W. Bohn, *Annu. Rev. Phys. Chem.* **1993**, *44*, 37–60; b) *J-Aggregates* (Ed.: T. Kobayashi), World Scientific, Singapore, **1996**. In several cases, *J*-aggregates in the mesoscopic range have been observed: c) H. Stegemeyer, F. Stöckel, *Ber. Bunsenges. Phys. Chem.* **1996**, *100*, 9–14; d) W. J. Harrison, D. L. Mateer, G. J. T. Tiddy, *J. Phys. Chem.* **1996**, *100*, 2310–2321; e) H. v. Berlepsch, C. Böttcher, A. Ouart, C. Burger, S. Dähne, S. Kirstein, *J. Phys. Chem. B* **2000**, *104*, 5255–5262.

[31] a) E. S. Emerson, M. A. Conlin, A. E. Rosenoff, K. S. Norland, H. Rodriguez, G. R. Bird, *J. Phys. Chem.* **1967**, *71*, 2396–2403; b) V. Czikkely, H. D. Försterling, H. Kuhn, *Chem. Phys. Lett.* **1970**, *6*, 11–14, 207–210; c) F. Dietz, *J. Signalaufzeichnungsmater.* **1973**, *1*, 157–180; F. Dietz, *J. Signalaufzeichnungsmater.* **1973**, *1*, 237–252; F. Dietz, *J. Signalaufzeichnungsmater.* **1973**, *1*, 381–382; d) E. Daltrozzo, G. Scheibe, K. Gschwind, F. Haimerl, *Photogr. Sci. Eng.* **1974**, *18*, 441–450.

[32] H. Langhals, R. Ismael, *Eur. J. Org. Chem.* **1998**, 1915–1917.

[33] a) D. Adam, P. Schuhmacher, J. Simmerer, L. Häussling, K. Siemensmeyer, K.-H. Etzbach, H. Ringsdorf, D. Haarer, *Nature* **1994**, *371*, 141–143; b) J. Simmerer, B. Glüsen, W. Paulus, A. Kettner, P. Schuhmacher, D. Adam, K.-H. Etzbach, K. Siemensmeyer, J. H. Wendorff, H. Ringsdorf, D. Haarer, *Adv. Mater.* **1996**, *8*, 815–819; c) T. Christ, B. Glüsen, A. Greiner, A. Kettner, R. Sander, V. Stümpflen, V. Tsukruk, J. H. Wendorff, *Adv. Mater.* **1997**, *9*, 48–52; d) K.-Y. Law, in *Handbook of Organic Conductive Molecules and Polymers*, *Vol. 1* (Ed.: H. S. Nalwa), Wiley, Chichester, **1997**, pp. 487–551; e) A. N. Cammidge, R. J. Bushby, in *Handbook of Liquid Crystals*, *Vol. 2B*: *Low Molecular Weight Liquid Crystals II* (Eds.: D. Demus, J. Goodby, G. W. Gray, H.-W. Spiess, V. Vill), Wiley-VCH, Weinheim, **1998**, pp. 693–743; f) S. Chandrasekhar in *Handbook of Liquid Crystals*, *Vol. 2B*: *Low Molecular Weight Liquid Crystals II* (Eds.: D. Demus, J. Goodby, G. W. Gray, H.-W. Spiess, V. Vill), Wiley–VCH, Weinheim, **1998**, pp. 749–777; g) H. Eichhorn, *J. Porphyrins Phthalocyanines* **2000**, *4*, 88–102; h) J. Kopitzke, J. H. Wendorff, *Chem. Unserer Zeit* **2000**, *34*, 4–16.

[34] a) P. Panayotatos, D. Parikh, R. Sauers, G. Bird, A. Piechowski, S. Husain, *Solar Cells* **1986**, *18*, 71–84; b) D. Wöhrle, D. Meissner, *Adv. Mater.* **1991**, *3*, 129–138; c) K.-Y. Law, *Chem. Rev.* **1993**, *93*, 449–486; d) G. Horowitz, F. Kouki, P. Spearman, D. Fichou, C. Nogues, X. Pan, F. Garnier, *Adv. Mater.* **1996**, *8*, 242–244; e) B. A. Gregg, J. Sprague, M. W. Peterson, *J. Phys. Chem. B* **1997**, *101*, 5362–5369.

[35] D. D. Perrin, W. L. F. Armarego, *Purification of Laboratory Chemicals*, 2nd ed., Pergamon Press, Oxford, **1980**.

[36] J. R. Lakowicz, *Principles of Fluorescence Spectroscopy*, 2nd ed., Kluwer Academic/Plenum Publishers, New York, **1999**, pp. 52–53.

[37] *CRC Handbook of Chemistry and Physics* (Ed.: D. R. Lide), 72nd ed., CRC Press, Boca Raton, FL, **1991**.

[38] J. R. Lakowicz, *Principles of Fluorescence Spectroscopy*, 2nd ed., Kluwer Academic/Plenum Publishers, New York, **1999**, pp. 53–55.

Received: November 3, 2000 [F2844]